

1 **Mathematical modelling elucidates core mechanisms** 2 **underpinning GnRH pulse generation**

3
4 Margaritis Voliotis^{1,2,*†}, Xiao Feng Li^{3, †}, Ross De Burgh^{3,†}, Geffen Lass³, Stafford L Lightman⁴,
5 Kevin T. O’Byrne³, Krasimira Tsaneva-Atanasova^{1,2,*}

6 ¹ Department of Mathematics and Living Systems Institute, College of Engineering, Mathematics and
7 Physical Sciences, University of Exeter, Exeter, EX4 4QF, UK.

8 ² EPSRC Centre for Predictive Modelling in Healthcare, University of Exeter, Exeter, EX4 4QJ, UK.

9 ³ Department of Women and Children’s Health, School of Life Course Sciences, King’s College
10 London, London SE1 1UL, UK.

11 ⁴ Henry Wellcome Laboratory for Integrative Neuroscience and Endocrinology, University of Bristol,
12 Bristol, BS1 3NY, UK.

13
14 * For correspondence: M.Voliotis@exeter.ac.uk, K.Tsaneva-Atanasova@exeter.ac.uk

15 † These authors contributed equally to this work

16 **Summary** (max 150 words)

17 Fertility critically depends on the gonadotropin-releasing hormone (GnRH) pulse generator, a
18 neural construct comprised of hypothalamic neurons co-expressing kisspeptin, neurokinin-B and
19 dynorphin that drives the pulsatile release of GnRH. How this neural network generates and
20 controls the appropriate ultradian frequency essential for gametogenesis and ovulation is unknown.
21 Here, we present a mathematical model of the GnRH pulse generator with theoretical evidence and
22 *in vivo* experimental data showing that robust pulsatile release of luteinizing hormone, a proxy
23 for GnRH, emerges abruptly as we increase the basal activity of the neuronal network using
24 continuous low frequency optogenetic stimulation of the neural construct. Further increases
25 in basal activity markedly increase pulse frequency. Model predictions that such behaviors
26 are concomitant of non-linear positive and negative feedback interactions mediated through
27 neurokinin-B and dynorphin signaling respectively are confirmed neuropharmacologically.
28 Our mathematical model sheds light on the long-elusive GnRH pulse generator offering new
29 horizons for fertility regulation.
30

31 **Introduction**

32 The periodic release of gonadotropin-releasing hormone (GnRH) plays a central role in control of
33 mammalian reproduction and is driven by hypothalamic neuronal networks (1). The operation of these
34 networks at a frequency appropriate for the species is critical for the generation of gonadotropin
35 hormone signals (luteinizing hormone, LH; and follicle-stimulating hormone, FSH) by the pituitary
36 gland, which stimulate the gonads and set in motion gametogenesis and ovulation. However, the
37 mechanisms underlying GnRH pulse generation and frequency control remain poorly understood.

38
39 Secretion of GnRH by GnRH neurons located in the hypothalamus into the pituitary portal circulation
40 is controlled by upstream hypothalamic signals (1). The neuropeptide kisspeptin has been identified as
41 a key regulator of GnRH secretion as both humans and rodents with inactivating mutations in
42 kisspeptin or its receptor fail to progress through puberty or show normal pulsatile LH secretion (2-4).

43 Within the hypothalamus, two major kisspeptin producing neuronal populations are found in the
44 arcuate nucleus (ARC) and in the preoptical area (5) or the anteroventral periventricular
45 (AVPV)/rostral periventricular (PeN) continuum in rodents (6). Moreover, the invariable association
46 between neuronal activity in the ARC and LH pulses across a range of species from rodents to primates
47 (7) has been suggestive that the ARC is the location of the GnRH pulse generator, and therefore the
48 ARC kisspeptin neurons, also known as KNDy for co-expressing neurokinin B (NKB) and dynorphin
49 (Dyn) alongside kisspeptin (8), constitute the core of the GnRH pulse generator.

50
51 Although animal studies have shown that KNDy neurons are critical for the regulation of GnRH
52 secretion, there has been relatively little understanding on the regulatory mechanisms involved in
53 generating and sustaining pulsatile dynamics. Pharmacological modulators of kisspeptin, NKB and
54 Dyn signaling have been extensively used to perturb the system and study the effect on the activity of a
55 hypothalamic neuronal population (using ARC multiunit activity (MUA) volleys, an
56 electrophysiological correlate of GnRH pulse generator activity, as a proxy) (9), as well as on
57 downstream GnRH/LH pulse dynamics (10-13). For example, it has been shown that kisspeptin (Kp-
58 10) administration does not affect MUA volleys in the ovariectomized rat (11), suggesting that
59 kisspeptin is relaying the pulsatile signal to GnRH neurons rather than generating it. On the contrary,
60 administration of NKB or Dyn modulates MUA volley frequency in the ovariectomized goat (13),
61 suggesting a more active role for these neuropeptides in the generation of the pulses. Deciphering,
62 however, the role of NKB has been problematic, and there exist conflicting data showing either an
63 increase or decrease of LH levels in response to administration of a selective NKB receptor (TACR3)
64 agonist (senktide) (10, 12, 14). Recently, a study combining optogenetics, with whole-cell
65 electrophysiology and molecular pharmacology has shed light on the action of the neuropeptides NKB
66 and Dyn in the KNDy network (15), with the key mechanistic finding that NKB functions as an
67 excitatory signal by depolarizing KNDy cells at the post-synaptic site, while co-released Dyn functions
68 pre-synoptically to inhibit NKB release.

69
70 Motivated by the experimental findings described above, we developed a mathematical model of the
71 ARC KNDy network. The model predicts that the KNDy population behaves as a relaxation oscillator:
72 autonomously generating and sustaining pulsatile activity similar to the hypothalamic MUA volleys
73 observed *in vivo* (9, 10). Model analysis reveals that *continuous* basal activity within the ARC KNDy
74 population as well as the positive and negative feedback interactions mediated by NKB and Dyn
75 signaling respectively are critical for pulsatility. We tested the model predictions *in vivo* using
76 optogenetics and showed that low-frequency *continuous* neuronal activation in the ARC KNDy
77 network initiates GnRH/LH pulsatility in female estrous mice and small changes in basal network
78 firing can have a large impact on pulse frequency. Furthermore, we showed that blocking NKB and
79 Dyn signaling alters the behavior of system in response to low-frequency *continuous* neuronal
80 activation in support of our modelling prediction.

81 **Results**

82 **A coarse-grained model of the ARC KNDy population**

83 We propose a new mathematical model (Fig. 1A) to study the dynamics of the ARC KNDy population.
84 The model is derived from a network description of the system (see SI) and describes the neuronal
85 population using three dynamical variables: \bar{D} , representing the average concentration of Dyn secreted
86 by the population; \bar{N} , representing the average concentration of NKB secreted by the population; and \bar{v} ,
87 representing the average firing activity of the population, measured in spikes/min. The dynamics of the
88 model variables are governed by the following set of coupled ordinary differential equations (ODEs):

$$\frac{d\bar{D}}{dt} = f_D(\bar{v}) - d_D\bar{D}; \quad [1]$$

$$\frac{d\bar{N}}{dt} = f_N(\bar{v}, \bar{D}) - d_N\bar{N}; \quad [2]$$

$$\frac{d\bar{v}}{dt} = f_v(\bar{v}, \bar{N}) - d_v\bar{v}. \quad [3]$$

89

90 Parameters d_D , d_N and d_v control the characteristic timescale of each variable. In particular, parameters
 91 d_D and d_N correspond to the rate at which Dyn and NKB are lost (e.g. due to diffusion or active
 92 degradation), while d_v relates to the rate at which neuronal activity resets to its basal level. Functions
 93 f_D , f_N describe the secretion rate of Dyn and NKB, respectively, while function f_v encodes how the
 94 firing rate changes in response to the current levels of NKB and firing rate.

95 We employ the following sigmoidal (Hill) functions to describe regulatory relationships between the
 96 variables. In particular, we set the secretion rate of Dyn and NKB to be:

$$f_D(\bar{v}) = k_{D,0} + k_D \frac{\bar{v}^{n_1}}{\bar{v}^{n_1} + K_{v,1}^{n_1}};$$

$$f_N(\bar{v}, \bar{D}) = k_{N,0} + k_N \frac{\bar{v}^{n_2}}{\bar{v}^{n_2} + K_{v,2}^{n_2}} \frac{K_D^{n_3}}{\bar{D}^{n_3} + K_D^{n_3}}.$$

97 In the equations above, both neuropeptides are constitutively secreted at rates $k_{D,0}$ and $k_{N,0}$. Neuronal
 98 activity further stimulates secretion of both neuropeptides, and Dyn represses secretion of NKB (15).
 99 Since the rate of neuropeptide release is inherently limited by availability of cytoplasmic secretory
 100 vesicles at the presynaptic terminals (16), we let secretion rates saturate at k_D and k_N , respectively. The
 101 effector levels at which saturation occurs are controlled via parameters $K_{v,1}$, $K_{v,2}$ and K_D . Furthermore,
 102 we set:

$$f_v(\bar{v}, \bar{N}) = v_0 \frac{1 - \exp(-I)}{1 + \exp(-I)};$$

$$I = I_0 + p_v \frac{N^{n_4}}{N^{n_4} + K_N^{n_4}} \bar{v},$$

103

104 where v_0 is the maximum rate at which the firing rate increases in response to synaptic inputs I . The
 105 stimulatory effect of NKB (which is secreted at the presynaptic terminal) is mediated via G protein-
 106 coupled receptor Tacr3 and is manifested as a short-term depolarization of the postsynaptic neuron
 107 (15). In the equation above, we accommodate this effect by letting a synaptic weight that is a sigmoidal
 108 function of NKB multiply \bar{v} . Parameter K_N sets the level of NKB at which its effect is half-maximal,
 109 and parameter p_v controls the strength of the synaptic connections between KNDy neurons. Finally,
 110 parameter I_0 controls the basal neuronal activity in the population, which could stem from synaptic
 111 noise or external inputs. We find that for biophysically relevant parameter values (see SI, Tbl. S1) the
 112 model reproduces the synchronized neuronal activity measured from the hypothalamus of
 113 ovariectomized rats (10). This finding further supports the hypothesis that KNDy neurons in the ARC
 114 constitute the core of the GnRH pulse generator.
 115

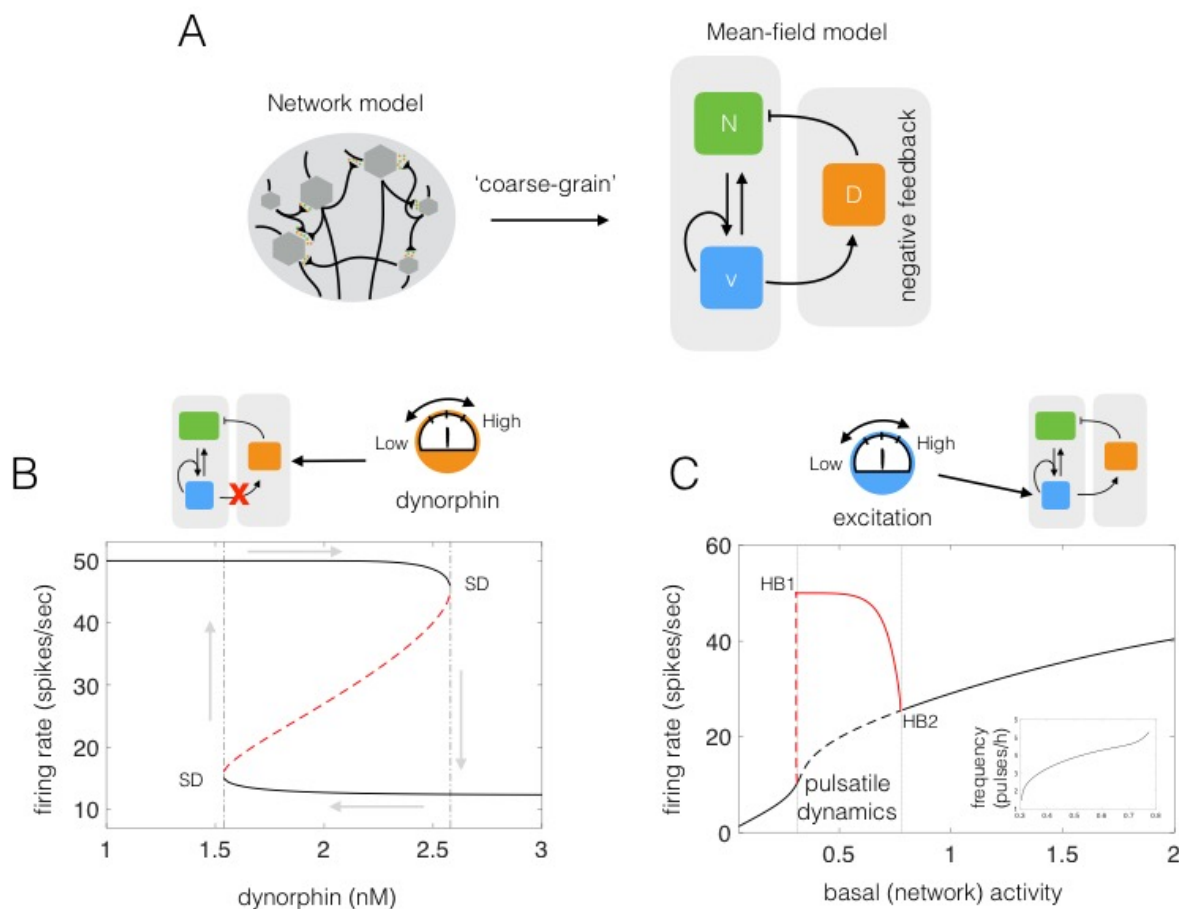
115

116 **Analysis of the model reveals the KNDy population functions as relaxation oscillator.**

117 Having shown that the model can reproduce sustained pulses of neuronal activity (see Fig. 1B), we
 118 proceed to investigate the mechanisms driving the phenomenon. We first focus on the role of Dyn-

119 mediated negative feedback using fast – slow analysis (17) of the coarse-grained model (Eqns. [1–3]).
 120 Model calibration suggests that Dyn operates at a slower time-scale than NKB (see SI). This time-scale
 121 separation, also supported by receptor internalization data (18), allows us to study the dynamics of the
 122 fast subsystem, comprised of \bar{N} and \bar{v} , as a function of the slow variable, \bar{D} , which is treated as a
 123 constant (bifurcation) parameter. Our analysis shows that for intermediate values of Dyn the fast
 124 subsystem can exist either in a high or a low activity state as demonstrated by the co-existing high and
 125 low branches of stable equilibria in Fig. 1B. This bi-stable behavior, stemming from the non-linear,
 126 positive feedback between neuronal activity and NKB secretion, leads to sustained oscillations of
 127 neuronal activity when combined with slow, Dyn-mediated, negative feedback. In engineering terms,
 128 the system behaves as a relaxation oscillator: where the bi-stable subsystem is successively excited
 129 (moved from low to high state) by external inputs or noise and silenced (moved from high to low state)
 130 as a result of negative feedback. We should note that a relatively slow negative feedback is sufficient
 131 for sustaining oscillations, however, the combination of negative feedback with bi-stability is found in
 132 many biological oscillators most likely because it confers robustness (19).
 133

134 Next, to demonstrate the role of basal neuronal activity within the KNDy network in the generation and
 135 modulation of oscillatory activity, we treat parameter I_0 as a bifurcation parameter. Our analysis shows
 136 that oscillatory behavior is supported within a critical range of I_0 values (see Fig. 1C). As I_0 is
 137 increased from zero, high-amplitude, low-frequency pulses emerge via a Hopf bifurcation (Fig. 1C;
 138 HB1 point). The frequency of pulses further increases with I_0 , until oscillations disappear via a Hopf
 139 bifurcation (Fig. 1C; HB2 point) and the system re-enters a silent (non-oscillatory) regime.

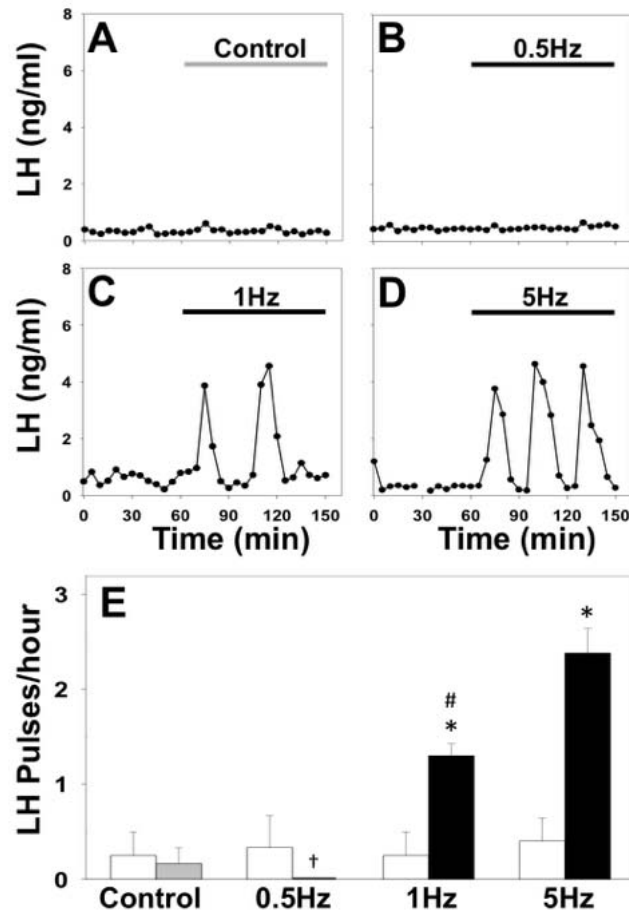


140
 141 **Figure 1: A coarse-grained model gives mechanistic insight into the pulsatile behavior of the ARC KNDy population.**
 142 (A) We derive a mean-field model of the neuronal population comprising three dynamical variables: \bar{D} , representing the

143 average concentration of Dyn secreted; \bar{N} , representing the concentration of NKB secreted; and \bar{v} , representing the average
144 firing activity of the neuronal population. (B) After disrupting the negative feedback loop (i.e., setting Dynorphin under
145 external control) the system exhibits, for intermediate values of Dynorphin, two stable equilibria (upper and lower solid
146 lines) and an unstable one (dashed red line). At the edges of the bi-stable regime equilibria are lost through a saddle-node
147 bifurcation (SD points). The bi-stability gives rise to hysteresis as the value of Dyn is varied externally (grey arrows). (C)
148 The coarse-grained model predicts how basal neuronal activity affects the system's dynamics and pulse frequency (inset).
149 As basal activity is increased from zero, high-amplitude, low-frequency pulses emerge after some critical value (HB1 point;
150 Hopf bifurcation). The frequency of pulses continues to increase with basal activity until oscillations disappear (HB2 point;
151 Hopf bifurcation) and the system enters a mono-stable regime (black solid line). The solid red line denotes the amplitude of
152 the pulses. Model parameter values are given in the SI (Tbl. S2).

153 **Continuous optogenetic stimulation of KNDy neurons generates pulsatile LH secretion *in vivo*.**

154 To test the model prediction that continuous excitation triggers pulsatile behavior of the system, we
155 stimulated the ARC KNDy population in Kiss-Cre mice (20) using optogenetics. ARC kisspeptin-
156 expressing neurons were transduced with a Cre-dependent adeno-associated virus (AAV9-EF1-dflox-
157 hChr2-(H134R)-mCherry-WPRE-hGH) to express channelrhodopsin (ChR2). AAV-injected, Kiss-Cre
158 mice were implanted with a fiber optic cannula in the ARC and the effects on LH pulsatility of
159 continuous stimulation at different frequencies was tested. After 1 h of controlled blood sampling, low-
160 frequency optic stimulation, 5-ms pulses of blue light (473 nm) at 0.5, 1 or 5 Hz, was initiated and
161 continuously delivered for 90 min. Control mice received no optic stimulation. During the course of the
162 experiment, blood samples (5 μ l) were collected every 5 min (20). To maximize the effect of
163 optogenetic stimulation, estrous mice were used which display minimum intrinsic pulse generator
164 activity (21). Indeed, the majority of the control non-optically stimulated Kiss-Cre mice in estrus
165 exhibited no LH pulse or intermittently 1 pulse during the 2.5 h sampling period (Fig. 2A&E).
166 Similarly, no LH pulses or occasionally 1 LH pulse was observed in the 60 min control period in the
167 optically stimulated mice (Fig. 2E; white bars). Optic stimulation at 0.5 Hz failed to induce LH pulses
168 (Fig. 2B&E). In contrast, increasing the low-frequency continuous stimulation to 1 Hz evoked regular
169 LH pulses (Fig. 2C&E, while 5 Hz resulted in a further, statistically significant ($p < 0.05$), increase in
170 LH pulse frequency (Fig. 2D&E), all in line with our theoretical predictions (Fig. 1C). Continuous
171 optogenetic stimulation (5 Hz) of AAV-injected wild-type C57BL/6 estrous mice ($n = 3$) failed to
172 induce LH pulses (data not shown) further confirming that increasing the basal activity in the ARC
173 KNDy neuronal population via low frequency continuous stimulation is sufficient to evoke and sustain
174 LH pulsatile dynamics.



175

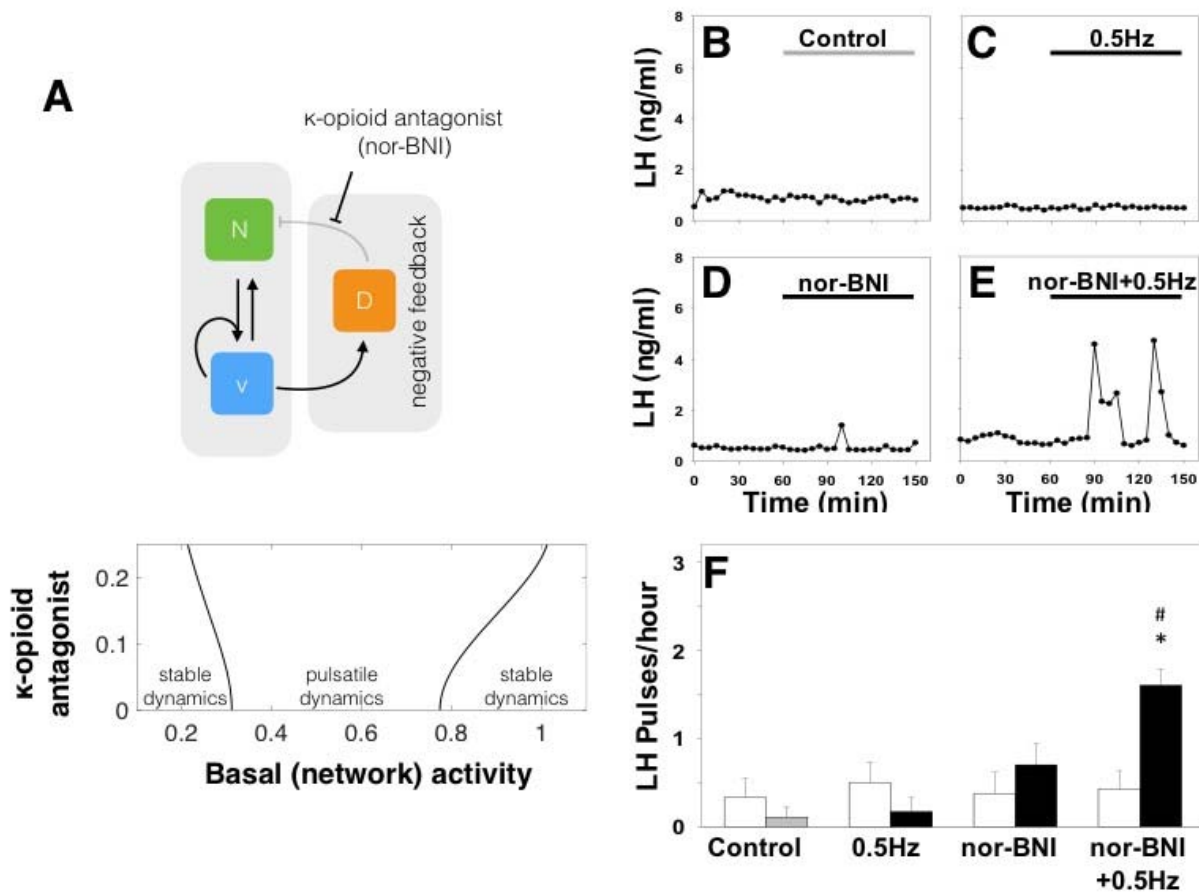
176 **Figure 2: Optic stimulation of ARC kisspeptin neurons triggers LH pulses in estrous Kiss-Cre mice.** (A-D)
177 Representative examples showing LH secretion in response to no stimulation (grey bar) as control (A), or continuous blue
178 light (473 nm, 5-ms pulse width, black bar) activation of kisspeptin neurons at 0.5 Hz (B), 1 Hz (C) or 5 Hz (D). (E)
179 Summary showing for each group mean \pm SEM LH pulse frequency over the 60min control period (white bars) and over the
180 subsequent stimulation period (black bars). * $P < 0.05$ vs pre-stimulation; # $P < 0.05$ vs stimulation at higher frequency.
181 †Absence of LH pulses in response to 0.5 Hz stimulation. $n = 4-6$ per group.

182 **Levels of Dyn and NKB signaling control the response of the system to optic stimulation.**

183 The above theoretical and experimental results reveal a characteristic tipping-point behavior of the
184 system, where a small increase in the basal activation levels is sufficient to trigger robust pulsatile
185 dynamics (22). Our model predicts that such behavior emerges as a result of the non-linear positive and
186 negative feedback interactions that are mediated through NKB and Dyn signaling respectively.
187 Therefore to test the active role of NKB and Dyn signaling on pulse generation, we next combined
188 optogenetic stimulation with neuropharmacological perturbations of the two pathways.

189 **Disrupting Dyn signaling increases the sensitivity of the system to optic stimulation.** Our model
190 predicts that disruption of Dyn signaling should enable pulsatile dynamics over a wider range of optic
191 stimulation frequencies (Fig. 3A). Intuitively, such disruption will reduce the strength of negative
192 feedback in the system and consequently lower optic stimulation frequencies would suffice to excite
193 the bi-stable neuronal population and set the relaxation oscillator in motion. To test this prediction *in-*

194 *in vivo* we repeated the optogenetic stimulation protocol at 0.5Hz together with nor-binaltorphimine (nor-
 195 BNI), a selective kappa opioid receptor (KOR) antagonist, to block Dyn signaling. Although 0.5Hz had
 196 previously failed to induce LH pulses (Fig. 4C&F), the addition of nor-BNI (bolus intra-
 197 cerebroventricular injection of 1.06 nmol over 5 min, followed by a continuous infusion of 1.28 nmol
 198 over 90 min) evokes a statistically significant increase in LH pulse frequency to approximately 1.6
 199 pulses/hour (Fig. 3F). Intra-cerebroventricular injection of nor-BNI alone had no effect on LH pulse
 200 frequency (Fig. 3D&F).



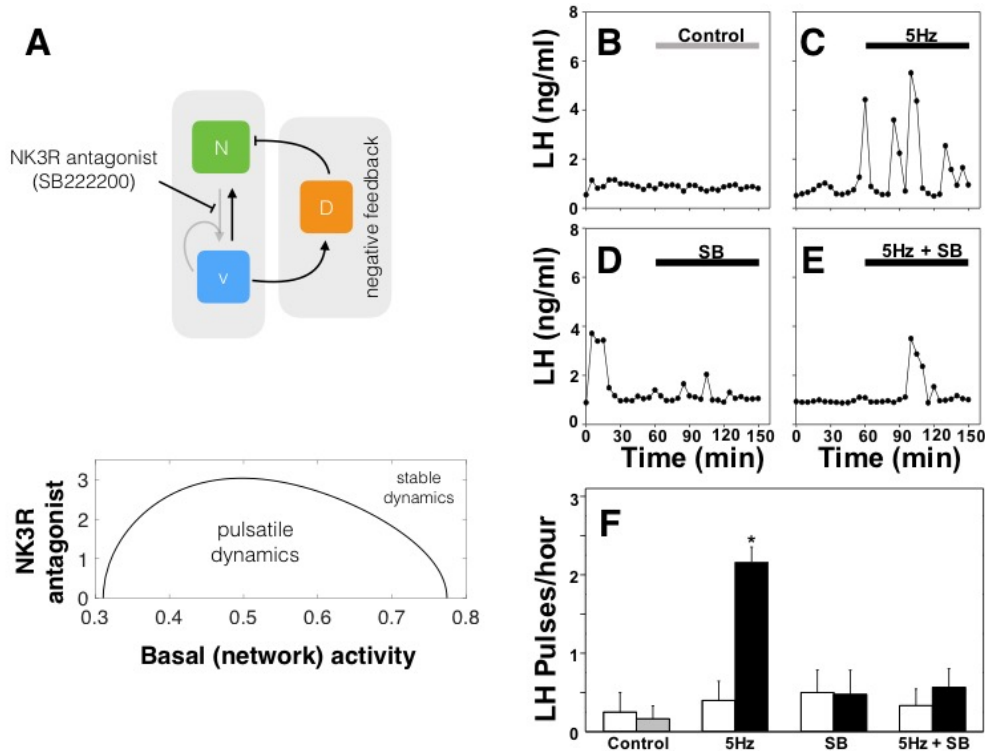
201

202 **Figure 3: Disrupting Dyn signaling increases the sensitivity of the system to optic stimulation.** (A) The model predicts
 203 that reducing the strength of negative feedback by partially blocking Dyn signaling should enable pulsatile dynamics over a
 204 wider range of optic stimulation frequencies. Nor-BNI, a Dyn receptor (kappa-opioid) antagonist, was used to block Dyn
 205 signaling *in-vivo*. (B-F) Representative examples showing LH secretion in response to no treatment (grey bar) as control
 206 (B), continuous blue light (473 nm, 5-ms pulse width, black bar) activation of kisspeptin neurons at 0.5 Hz (C), nor-BNI
 207 treatment (bolus intra-cerebroventricular injection of 1.06 nmol over 5 min, followed by a continuous infusion of 1.28 nmol
 208 over 90 min) (D) combined nor-BNI treatment and optic stimulation at 0.5Hz (E). (F) Summary plot showing for each group
 209 mean±SEM LH pulse frequency over the pre-treatment (white bars) and treatment period (black bars). *P < 0.05 vs pre-
 210 treatment; #P < 0.05 vs only optic stimulation treatment. n = 4-6 per group.

211

212 **Disrupting NKB signaling desensitizes the system to optic stimulation.** Our model predicts that
 213 disruption of NKB signaling should desensitize the system to external optic stimulation (see Fig. 4A).
 214 NKB signaling is key for pulsatile behavior as it enables positive feedback interactions within the
 215 population and therefore promotes bi-stability. Hence disrupting NKB signaling ought to decrease the

216 propensity of the system to get excited into the pulsatile regime by external stimulation. To test this
217 prediction *in-vivo* we repeated the optogenetic stimulation protocol at the highest frequency (5Hz), and
218 used SB222200, a selective TACR3 antagonist, to block NKB signaling. Although 5Hz had previously
219 induced a high frequency LH response (Fig. 4C&F), we observe that antagonist addition (bolus intra-
220 cerebroventricular injection of 6 nmol over 5 min, followed by a continuous infusion of 9 nmol over 90
221 min) completely blocked the increased LH pulse frequency (Fig. 4E&F). Intra-cerebroventricular
222 injection of SB222200 alone had no effect on LH pulse frequency (Fig. 4D&F).



223

224 Figure 4: **Disrupting NKB signaling desensitize the system to optic stimulation.** (A) The model predicts that weakening
225 bi-stability by blocking NKB signaling should restrict the range of optic stimulation frequencies that trigger pulsatility.
226 SB222200 (SB), an NKB receptor (TACR3) antagonist, was used to block NKB signaling *in-vivo*. (B-F) Representative
227 examples showing LH secretion in response to no treatment (grey bar) as control (B), continuous blue light (473 nm, 5-ms
228 pulse width, black bar) activation of kisspeptin neurons at 5 Hz (C), SB222200 treatment (bolus intra-cerebroventricular
229 injection of 6 nmol over 5 min, followed by a continuous infusion of 9 nmol over 90 min) (D) combined SB222200
230 treatment and optic stimulation at 0.5Hz (E). (F) Summary plot showing for each group mean \pm SEM LH pulse frequency
231 over the pre-treatment (white bars) and treatment period (black bars). *P < 0.05 vs pre-treatment. n = 4-6 per group.

232 Discussion

233 Motivated by recent experimental evidence, we developed and studied a mathematical model of the
234 KNDy neural population in the ARC, a population proposed to comprise the core of the GnRH pulse
235 generator (23, 24). Our model demonstrates that the KNDy population can indeed produce and sustain
236 pulsatile dynamics working as a relaxation oscillator. On the one hand, auto-stimulation via NKB
237 signaling allows the population to behave as a bi-stable switch, firing either at a high or low rate.
238 Moreover, basal neuronal activity and negative feedback through Dyn signaling allow the population to
239 switch between the two activity states in a regular manner, giving rise to pulses of neuronal activity.
240 Using global sensitivity analysis, we found that this mechanism of pulse generation is robust to
241 parameter perturbations (SI, Fig. S3). In fact, co-variation of parameters governing, for example, the

242 magnitude of basal activity, and the maximum secretion rates of NKB and Dyn is a more effective way
243 of modulating the systems' oscillatory behavior (amplitude and frequency). This multi-channel mode
244 of efficient regulation is perhaps not surprising given the system's crucial function, and hints that
245 steroid feedback modulating the dynamics of the pulse generator over the reproductive cycle in female
246 mammals is mediated through multiple, possibly interlinked, pathways.

247
248 Following model predictions, we explored the effect of continuous optogenetic activation of the KNDy
249 population on LH pulse dynamics, a proxy for GnRH pulse dynamics. The model predicts that pulsatile
250 dynamics of the system critically depend on the levels of basal activity in the KNDy population, and
251 highlights the tipping-point behavior of the system as basal activity is modulated. For example, starting
252 from a silent state of the system, introducing low levels of basal activity can reinstate pulses and
253 increase their frequency. We have tested these model predictions *in-vivo* using optogenetics (24-26),
254 and showed that we are able to directly control the generation and frequency of LH pulses in estrous
255 mice by selectively exciting KNDy neurons in a continuous fashion at 1Hz and 5Hz. It is important to
256 note that the model has informed the design of the experiments by suggesting the use of low-frequency
257 optic stimulation for the first time in investigating LH pulse generation and in contrast to previous
258 studies (24-26). Our results suggest that inhibitory or excitatory synaptic signaling within the KNDy
259 neural population have a drastic effect on GnRH/LH pulse dynamics. We speculate that this enables
260 KNDy neurons to integrate and transmit information regarding the overall state of the organism that is
261 relevant for reproduction: for example, information on the emotional state and stress level through
262 synaptic connections originating at the level of the amygdala (27), a key limbic brain structure; or
263 information regarding the nutritional state of the organism through connections from Agouti-related
264 peptide (AgRP)-expressing neurons in the hypothalamus (28).

265
266 The model predicted that the systems' pulsatile behavior emerges as a result of the non-linear positive
267 and negative feedback interactions that are mediated through NKB and Dyn signaling respectively.
268 Using experimental protocol suggested by model analysis we showed that the response of the system to
269 external optic stimulation indeed follows our NKB and Dyn signaling predictions. Our results highlight
270 the need for a quantitative understanding of how the sex-steroid milieu affects the NKB and Dyn
271 signaling pathways in the KNDy population. Such an understanding will lead to more accurate
272 interpretation of results from *in-vivo* neuropharmacological perturbation experiments in various animal
273 models and will shed light on the mechanisms underlying the regulation of pulsatile LH secretion in
274 various natural settings such as lactational amenorrhoea or pharmaceutical interventions including the
275 hormone contraceptive pill. We envision that as hormonal measurement techniques advance, enabling
276 accurate, real-time readouts from individuals at low cost, such predictive mathematical models would
277 be a valuable tool for understanding of reproductive physiopathology.

278 **Materials and methods**

279 **Bifurcation analysis and numerical experiments**

280 Bifurcation analysis of the coarse-grained model was performed using AUTO-07p (29). Both the full
281 network model and coarse-grained model were simulated in Matlab using function ode45 (explicit
282 Runge-Kutta (4, 5) solver).

283 **Animals**

284 Breeding pairs of Kiss-Cre heterozygous transgenic mice (30) were obtained from the Department of
285 Physiology, Development and Neuroscience, University of Cambridge, UK. Litters from the breeding
286 pairs were genotyped by polymerase chain reaction (PCR) analysis. Adult female mice (8-14 wk old;

287 25-30g) heterozygous for the Kiss-Cre transgene or wild-type C57BL/6 littermates, with normal
288 pubertal development and estrous cyclicity, were used. Mice were housed under a 12:12 h light/dark
289 cycle (lights on 0700 h) at 22 ± 2 °C and provided with food (standard maintenance diet; Special
290 Dietary Services, Witter, UK) and water ad libitum. All animal procedures performed were approved
291 by the Animal Welfare and Ethical Review Body (AWERB) Committee at King's College London, and
292 in accordance with the UK Home Office Regulations.

293 **Surgical procedures**

294 Surgical procedures for stereotaxic injection of AAV9-EF1-dflox-hChR2-(H134R)-mCherry-WPRE-
295 hGH (4.35 x 10¹³ GC/ml; Penn Vector Core) to express channelrhodopsin (ChR2) in ARC kisspeptin
296 neurons were performed under aseptic conditions with general anesthesia induced by ketamine
297 (Vetalar, 100 mg/kg, i.p.; Pfizer, Sandwich, UK) and xylazine (Rompun, 10 mg/kg, i.p.; Bayer,
298 Leverkusen, Germany). Kiss-Cre female mice (n = 7) or wide-type (n = 3) were secured in a David
299 Kopf Motorized stereotaxic frame and surgical procedures were performed using a Robot Stereotaxy
300 system (Neurostar, Tübingen, Germany). A small hole was drilled into the skull at a location above the
301 ARC. The stereotaxic injection coordinates used to target the ARC were obtained from the mouse
302 brain atlas of Paxinos and Franklin (31) (0.3 mm lateral, 1.2 mm posterior to bregma and at a depth of
303 6.0 mm). Using a 2- μ L Hamilton micro-syringe (Esslab, Essex, UK) attached to the Robot Stereotaxy,
304 1 μ l of the AAV-construct was injected unilaterally into the ARC at a rate of 100 nl/min. The needle
305 was left in position for a further 5 min and then removed slowly over 1 min. A fiber optic cannula (200
306 μ m, 0.39NA, 1.25mm ceramic ferrule; Thorlabs LTD, Ely, UK) was then inserted at the same co-
307 ordinates as the injection site, but to a depth of 5.88 mm, so that the fiber optic cannula was situated
308 immediately above the latter. Dental cement or a glue composite was then used to fix the cannula in
309 place, and the skin incision closed with suture. A separate group of mice (n = 10) injected with the
310 AAV construct, and fiber optic cannulae as described above, but additionally chronically implanted
311 with an intra-cerebroventricular (icv) fluid cannulae (26 gauge; Plastics One, Roanoke, VA, USA)
312 targeting the lateral ventricle (coordinates: 1.1 mm lateral, 1.0 mm posterior to bregma and at a depth
313 of 3.0 mm), was used for the combined neuropharmacological and optogenetic studies. After surgery,
314 mice were left for 4 weeks to achieve effective opsin expression. After a 1-wk recovery period, the
315 mice were handled daily to acclimatize them to the tail-tip blood sampling procedure (32).

316 **Experimental design, and blood samplings for LH measurement**

317 Prior to optogenetic stimulation, the very tip of the mouse's tail was excised using a sterile scalpel for
318 subsequent blood sample collection (21). The chronically implanted fiber optic cannula was then
319 attached via a ceramic mating sleeve to a multimode fiber optic rotary joint patch cables (Thorlabs),
320 allowing freedom of movement of the animal, for delivery of blue light (473 nm wavelength) using a
321 Grass SD9B stimulator controlled DPSS laser (Laserglow Technologies, Toronto, Canada). Laser
322 intensity at the tip of the fiber optic patch cable was 5 mW. After 1 h acclimatization, blood samples
323 (5 μ l) were collected every 5 min for 2.5 h. After 1 h controlled blood sampling, continuous optic
324 stimulation (5-ms pulse width) was initiated at 0.5, 1 or 5 Hz for 90 min. Controls received no optic
325 stimulation. Kiss-Cre mice received the stimulation protocols in random order. Wild-type received 5
326 Hz optic stimulation only.

327
328 For the neuropharmacological manipulation of Dyn or NKB signaling with or without simultaneous
329 optogenetic stimulation the animals were appropriately prepared as described above, but in addition an
330 icv injection cannula with extension tubing, preloaded with drug solution (nor-BNI or SB222200
331 dissolved in artificial cerebrospinal fluid), was inserted into the guide cannula immediately after
332 connection of the fiber optic cannula. The tubing was extended outside the cage and connected to a 10
333 μ l syringe (Hamilton) mounted in an automated Harvard pump (Harvard Apparatus, Holliston, MA,

334 USA) to allow remote microinfusion without disturbing the mice during the experiment. Five min
335 before optic stimulation, icv administration of drug treatment commenced as a bolus injection over 5
336 min, followed by a continuous infusion for the remainder of the experiment. In the absence of optic
337 stimulation the same icv regimen was used. The blood samples were processed by ELISA as reported
338 previously (32). Mouse LH standard and antibody were purchased from Harbour-UCLA, USA, and
339 secondary antibody (NA934) was from VWR International, UK. The intra-assay and inter-assay
340 variations were 4.6% and 10.2%, respectively.

341 **Validation of AAV injection site**

342 After completion of experiments, mice were anaesthetized with a lethal dose of ketamine and
343 transcardially perfused with heparinized saline for 5 min, followed by 10 min of ice-cold 4%
344 paraformaldehyde (PFA) in phosphate buffer (pH 7.4) for 15 min using a pump (Minipuls, Gilson,
345 Villiers Le Bel, France). Brains were rapidly collected and postfixed sequentially at 4 °C in 15%
346 sucrose in 4% PFA and in 30% sucrose in phosphate-buffered saline until they sank. Afterwards, brains
347 were snap-frozen on dry ice and stored at -80 °C until processing. Brains were coronally sectioned (40-
348 µm) using a cryostat (Bright Instrument Co., Luton, UK) and every third section was collected between
349 -1.34 mm to -2.70 mm from the bregma. Sections were mounted on microscope slides, air-dried and
350 cover slipped with ProLong Antifade mounting medium (Molecular Probes, Inc. OR, USA). The
351 injection site was verified and evaluated using Axioskop 2 Plus microscope equipped with axiovision
352 4.7 (see also SI, Fig. S1). One of 17 Kiss-Cre mice failed to show mCherry fluorescence in the ARC
353 and was excluded from the analysis.

354 **LH Pulses and Statistical Analysis**

355 Detection of LH pulses was established by use of the Dynpeak algorithm (33). The effect of
356 optogenetic stimulation on parameters of LH secretion was calculated by comparing the mean number
357 of LH pulse per hour, within the 90 min stimulation/drug delivery period with the 60 min pre-
358 stimulation/drug delivery control period. For the non-stimulated control animals, the same timepoints
359 were compared. The mean number of LH pulse per hour, within the 90 min stimulation period, or
360 equivalent, was also compared between experimental groups. Statistical significance was tested using
361 one-way ANOVA followed by Dunnett's test. $P < 0.05$ was considered statistically significant. Data
362 are presented as the mean \pm SEM.

363 **Supporting information**

364 **S1 text.**

365 **Supporting Information.**

366 **Acknowledgments**

367 KTA and MV gratefully acknowledge the financial support of the EPSRC via grant EP/N014391/1.
368 KOB and SLL gratefully acknowledge the financial support of the MRC via grant MR/N022637/1.

369 **References**

- 370 1. Herbison AE (2016) Control of puberty onset and fertility by gonadotropin-releasing hormone
371 neurons. *Nature Reviews Endocrinology* 12(8):452-466.
- 372 2. de Roux N, *et al.* (2003) Hypogonadotropic hypogonadism due to loss of function of the
373 KiSS1-derived peptide receptor GPR54. *Proceedings of the National Academy of Sciences*
374 100(19):10972-10976.

- 375 3. Kaiser UB (2015) Understanding reproductive endocrine disorders. *Nature Reviews*
376 *Endocrinology* 11(11):640-641.
- 377 4. Seminara SB, *et al.* (2003) The GPR54 Gene as a Regulator of Puberty. *New England Journal of*
378 *Medicine* 349(17):1614-1627.
- 379 5. Hrabovszky E (2014) Neuroanatomy of the Human Hypothalamic Kisspeptin System.
380 *Neuroendocrinology* 99(1):33-48.
- 381 6. Clarkson J, Danglemont de Tassigny X, Colledge WH, Caraty A, & Herbison AE (2009)
382 Distribution of Kisspeptin Neurons in the Adult Female Mouse Brain. *Journal of*
383 *Neuroendocrinology* 21(8):673-682.
- 384 7. Plant TM & Zeleznik AJ (2014) *Knobil and Neill's physiology of reproduction* (Academic
385 Press).
- 386 8. Lehman MN, Coolen LM, & Goodman RL (2011) Minireview: Kisspeptin/Neurokinin
387 B/Dynorphin (KNDy) Cells of the Arcuate Nucleus: A Central Node in the Control of
388 Gonadotropin-Releasing Hormone Secretion. *Endocrinology*.
- 389 9. Wilson RC, *et al.* (1984) Central electrophysiologic correlates of pulsatile luteinizing hormone
390 secretion in the rhesus monkey. *Neuroendocrinology* 39(3):256-260.
- 391 10. Kinsey-Jones JS, *et al.* (2011) The Inhibitory Effects of Neurokinin B on GnRH Pulse
392 Generator Frequency in the Female Rat. *Endocrinology* 153(1):307-315.
- 393 11. Kinsey-Jones JS, Li XF, Luckman SM, & O'Byrne KT (2008) Effects of Kisspeptin-10 on the
394 Electrophysiological Manifestation of Gonadotropin-Releasing Hormone Pulse Generator
395 Activity in the Female Rat. *Endocrinology* 149(3):1004-1008.
- 396 12. Navarro VM, *et al.* (2009) Regulation of Gonadotropin-Releasing Hormone Secretion by
397 Kisspeptin/Dynorphin/Neurokinin B Neurons in the Arcuate Nucleus of the Mouse. *The*
398 *Journal of Neuroscience* 29(38):11859-11866.
- 399 13. Wakabayashi Y, *et al.* (2010) Neurokinin B and Dynorphin A in Kisspeptin Neurons of the
400 Arcuate Nucleus Participate in Generation of Periodic Oscillation of Neural Activity Driving
401 Pulsatile Gonadotropin-Releasing Hormone Secretion in the Goat. *The Journal of Neuroscience*
402 30(8):3124-3132.
- 403 14. Sandoval-Guzmán T & E Rance N (2004) Central injection of senktide, an NK3 receptor
404 agonist, or neuropeptide Y inhibits LH secretion and induces different patterns of Fos
405 expression in the rat hypothalamus. *Brain research* 1026(2):307-312.
- 406 15. Qiu J, *et al.* (2016) High-frequency stimulation-induced peptide release synchronizes arcuate
407 kisspeptin neurons and excites GnRH neurons. *eLife* 5:e16246-e16246.
- 408 16. Han W, Ng Y-K, Axelrod D, & Levitan ES (1999) Neuropeptide release by efficient
409 recruitment of diffusing cytoplasmic secretory vesicles. *Proceedings of the National Academy*
410 *of Sciences* 96(25):14577-14582.
- 411 17. Rinzel J (1985) Bursting oscillations in an excitable membrane model. *Ordinary and partial*
412 *differential equations*, (Springer), pp 304-316.
- 413 18. Weems PW, *et al.* (2018) Evidence That Dynorphin Acts Upon KNDy and GnRH Neurons
414 During GnRH Pulse Termination in the Ewe. *Endocrinology* 159(9):3187-3199.
- 415 19. Pomeroy JR, Sontag ED, & Ferrell JE (2003) Building a cell cycle oscillator: hysteresis and
416 bistability in the activation of Cdc2. *Nature Cell Biology* 5(4):346-351.
- 417 20. Adekunbi D, *et al.* (2018) Kisspeptin neurons in the posterodorsal medial amygdala modulate
418 sexual partner preference and anxiety in male mice. *Journal of neuroendocrinology*
419 30(3):e12572.
- 420 21. Czieselsky K, *et al.* (2016) Pulse and surge profiles of luteinizing hormone secretion in the
421 mouse. *Endocrinology* 157(12):4794-4802.
- 422 22. Strogatz SH (2018) *Nonlinear dynamics and chaos: with applications to physics, biology,*
423 *chemistry, and engineering* (CRC Press).

- 424 23. Fergani C & Navarro VM (2017) Expanding the role of tachykinins in the neuroendocrine
425 control of reproduction. *Reproduction* 153(1):R1-R14.
- 426 24. Clarkson J, *et al.* (2017) Definition of the hypothalamic GnRH pulse generator in mice.
427 *Proceedings of the National Academy of Sciences* 114(47):E10216-E10223.
- 428 25. Campos P & Herbison AE (2014) Optogenetic activation of GnRH neurons reveals minimal
429 requirements for pulsatile luteinizing hormone secretion. *Proceedings of the National Academy*
430 *of Sciences* 111(51):18387-18392.
- 431 26. Han SY, McLennan T, Czieselsky K, & Herbison AE (2015) Selective optogenetic activation of
432 arcuate kisspeptin neurons generates pulsatile luteinizing hormone secretion. *Proceedings of the*
433 *National Academy of Sciences* 112(42):13109-13114.
- 434 27. Lin Y, *et al.* (2010) The role of the medial and central amygdala in stress-induced suppression
435 of pulsatile LH secretion in female rats. *Endocrinology* 152(2):545-555.
- 436 28. Padilla SL, *et al.* (2017) AgRP to Kiss1 neuron signaling links nutritional state and fertility.
437 *Proceedings of the National Academy of Sciences*:201621065.
- 438 29. Doedel EJ, *et al.* (2007) AUTO-07P: Continuation and bifurcation software for ordinary
439 differential equations.
- 440 30. Yeo SH, *et al.* (2016) Visualisation of Kiss1 Neurone Distribution Using a Kiss1-CRE
441 Transgenic Mouse. *Journal of neuroendocrinology* 28(11).
- 442 31. Paxinos G & Franklin K (2004) The mouse brain in stereotaxic coordinates Amsterdam.
443 (Boston, MA: Elsevier Academic Press).
- 444 32. Steyn FJ, *et al.* (2013) Development of a methodology for and assessment of pulsatile
445 luteinizing hormone secretion in juvenile and adult male mice. *Endocrinology* 154(12):4939-
446 4945.
- 447 33. Vidal A, Zhang Q, Médigue C, Fabre S, & Clément F (2012) DynPeak: An algorithm for pulse
448 detection and frequency analysis in hormonal time series. *PLoS One* 7(7):e39001.
- 449